Comparative solid state and solution NMR structural and dynamic studies on tetra- and higher-nuclearity transition metal carbonyl clusters

Taro Eguchi[a] and Brian T. Heaton[b]

[a] Department of Chemistry, Graduate School of Science, Osaka University, Toyonaka, Osaka 560-0043, Japan
[b] Department of Chemistry, University of Liverpool, Liverpool, UK L69 7ZD

Clusters provide interesting models for surfaces and sometimes provide a controlled step-wise sequence of cluster growth. Although the metal geometry in *homometallic* clusters can now be predicted reliably from electron counting rules, it is much more difficult to predict both the *metal site occupancy* in *heterometallic* clusters and the *carbonyl* and *non-carbonyl ligand site occupancies* on the metallic framework; this is especially true for the ubiquitous hydrogen and structural elucidation of these clusters has had to rely heavily on neutron diffraction and NMR measurements, which are particularly useful when the metal has a spin. Similarly, the ease of migration and the exact migrational pathway(s) of CO and/or H are also difficult to predict, although NMR measurements in solution often allow the detailed pathway of ligand migrations to be unambiguously established. The purpose of this Perspective is to compare and contrast the dynamic and structural information available from solid state multinuclear NMR measurements with data obtained from solution NMR and other related spectroscopic and structural measurements on tetra- and higher-nuclearity transition metal carbonyl clusters.

1 Introduction

Over the last 30 years there has been an explosion of interest in transition metal carbonyl cluster chemistry with a dramatic increase in both the size and variety of structurally characterised clusters. X-Ray analysis has been very important for their characterisation and the structure of the metal skeleton may now reliably be predicted from electron counting rules.[1,2] The developments in both NMR techniques and instrumentation have also been very important in this area. Solution NMR studies are particularly useful, especially if the cluster contains a metal with a spin (*e.g.* ^{103}Rh),[3] in establishing the following. (1) Structures in solution when X-ray quality crystals cannot be obtained. It is still impossible however, to *predict* the carbonyl distribution around the metallic skeleton, the site occupancy of different metals in heterometallic clusters and the site occupancy of non-carbonyl ligands (*e.g.* PR_3) in either homo- or hetero-metallic clusters and all of these can only be established by measurements on each individual cluster. (2) Hydride site occupancies. (3) Detailed pathways of ligand (H, CO) and/or metal migrations. There are fewer solid state NMR studies on transition metal carbonyl clusters, but they have provided:

Taro Eguchi

Brian T. Heaton

Table 1 Solution and solid state ^{13}CO chemical shifts for neutral metal carbonyl clusters containing ≥4 metal atoms

| Cluster | CO site | Solid state NMR | | Expected relative intensity from X-ray data | | Solution NMR | |
		Ref.	$\delta(CO)^a$	Solid	Solution	$\delta(CO)^a$	Ref.
$[Co_4(CO)_{12}]$	Terminal	7	198.4, 192.4, 183.7 178.9, 175.0, 163.8 ^{b}	^{c}	9	205 to 200, 195.6, 191.7	8
	μ		229.3 ^{b}	^{c}	3	243.1	
$[Rh_4(CO)_{12}]$	Terminal/apical	9	183.4(2), 179.2(1)	2:1	3	181.8(3) ^{d}	10
	Terminal/radial		184.0(2), 182.6(1)	2:1	3	183.4(3) ^{d}	
	Terminal/axial		175.4(2), 173.3(1)	2:1	3	175.5(3) ^{d}	
	μ		228(2), 226(1)	2:1	3	228.8(3) ^{d}	
$[Ir_4(CO)_{12}]$	Terminal	11	154.2 (br)	^{e}	12	156	12
$[Rh_6(CO)_{16}]$	Terminal	11	179.4(2), 180.1(2) 181.2(6), 182.4(2)	2:2:6:2	12	180.1(12)	13
	$μ_3$		229.1(2), 234.1(2)	2:2	4	231.5(4)	

^{a} Numbers in parentheses indicate intensities and br = broad. ^{b} Data at 25 °C. ^{c} Disorder prevented these data being obtained. ^{d} Data at −65 °C. ^{e} All the COs are inequivalent (see text).

structural information on ligand (H, CO)/metal site occupancies, dynamic information about ligand/metal migrations and information on the bonding of CO and interstitial elements from chemical shift anisotropy data.

The purpose of this review is to summarise the presently available solid state NMR measurements on tetra- and higher-nuclearity clusters which have yielded structural and/or dynamic information and to compare these measurements both with NMR data obtained in solution and other related structural and spectroscopic data. Clusters containing ≥4 metals are chosen since the conflicting views about the mechanism of CO fluxionality in solution for trinuclear clusters have recently been presented [4,5] and the reader is referred to these reviews and the recent summary by Farrugia [6] who compared solution and solid state measurements on trinuclear clusters, $[M_{3-x}M'_x(CO)_{12}]$ ($x = 0$, M = Fe, Ru or Os; $x = 1$, M = Fe, M' = Ru or Os; $x = 2$, M = Fe, M' = Ru).

The dynamic situation for trinuclear clusters is complicated by disorder problems of the M_3 triangle within the carbonyl icosahedral polyhedron, but variable temperature X-ray studies show that there is a reduction of this disorder at low temperature and, in some cases (Fe_2M', M' = Ru or Os), the system becomes completely ordered at low temperature. Solid state ^{13}C EXSY measurements on $[Fe_2Os(CO)_{12}]$ provide evidence for 60° jumps of the Fe_2Os triangle within the CO polyhedron together with a C_2 rotation of the $Os(CO)_4$ group; this latter rotation has the effect of interconverting the axial/equatorial COs on Os and both processes occur with similar activation energies (>42 kJ mol^{-1}). However, to have both of these motions occurring simultaneously seems to us highly unlikely. Furthermore, the migrational movements of clusters in the solid and solution state could reasonably be expected to be different and even if similar movements occur then different activation energies could reasonably be expected because of the different lattice constraints.

2 Non-substituted neutral carbonyl clusters

In the solid state, the carbonyl T_1 values of all clusters of this type are extremely long and, in order to enhance the signal-to-noise ratio, it is advantageous to: isotopically enrich with ^{13}CO to *ca.* 30%; higher enrichments cause broadening of the resonances due to the introduction of $^nJ(C–C')$ ($n = 2$ or 3); use high field spectrometers. The clusters studied by ^{13}C MAS NMR are shown, together with the solution data, in Table 1.

There have been few solid state NMR measurements on neutral unsubstituted clusters containing ≥4 metals but, in the absence of exchange and/or interaction with a quadrupolar nucleus, see below, the solid state NMR spectra usually have: an isotropic ^{13}C chemical shift for *each crystallographically distinct carbonyl site* with the average value being similar to that obtained in solution; coupling constants, *e.g.* $^1J(^{103}Rh–^{13}CO)$, that are similar to those observed in solution and can usually be resolved when ≥30 Hz.

It should be noted that relative ratios of different resonances in solid state NMR spectra can only be obtained through integration of *all* the spinning side bands and this becomes very difficult for clusters which contain terminal and face-bridging ($μ_3$) CO resonances, *e.g.* $[Rh_6(CO)_{16}]$; it has been shown that the $μ_3$-COs give rise to relatively weak spinning sidebands (SSBs) because of the low anisotropy whereas more intense SSBs are observed for the terminal COs because of the much higher anisotropy,[11] see below.

Furthermore, CO fluxionality in the solid state generally seems to be more difficult than in solution as exemplified by $[Rh_4(CO)_{12}]$. Cotton *et al.*[14] first reported the intramolecular exchange of bridge/terminal COs for $[Rh_4(CO)_{12}]$ in solution. The limiting fast-exchange spectrum (59 °C) gives rise to a single resonance (δ 189.5) which consists of a quintet ("J" 17.2 Hz) due to a time-averaged coupling "J" of the exchanging COs with all the Rhs which have become equivalent through the exchange process.[14] At −65 °C the ^{13}C spectrum in solution is consistent with the static structure[15] and has been assigned by comparison with substituted derivatives of $[Rh_4(CO)_{12}]$;[10] recent ^{13}C-{^{103}Rh} measurements by one of the authors have confirmed these earlier assignments of the low temperature ^{13}C NMR spectrum in solution. Comparison of solution and solid state 50 MHz ^{13}C NMR spectra at room temperature show that, whereas solution spectra are severely broadened due to CO fluxionality, solid state spectra are well resolved and consistent with the static structure.[9] Unfortunately, it was not possible to go to higher temperatures in the solid state measurements in order to induce CO fluxionality because of the ready conversion of $[Rh_4(CO)_{12}]$ into $[Rh_6(CO)_{16}]$. These results tend to support the merry-go-round process for CO fluxionality in solution. Following similar arguments used for other clusters,[16] the same process in the solid state would be expected to have much higher energy because of the gross reorganisation of the crystal lattice/volume and clearly does not occur in the solid state. Similarly, the reorientation of the metal polyhedron within the CO polyhedron, which occurs for $[Co_4(CO)_{12}]$ in the solid state, see below, does *not* occur for $[Rh_4(CO)_{12}]$ in the solid state.

The compound $[Ir_4(CO)_{12}]$ has only terminal COs and, consistent with the T_d symmetry, has a single ^{13}C resonance in solution[12] (see Table 1). However, its solid state structure[17] contains three distinct molecules, each with C_3 symmetry, which should give rise to 12 distinct ^{13}CO resonances in the solid state

spectrum but only one rather broad resonance is observed[11] (see Table 1). This poor resolution is attributed to dipolar coupling between ^{13}C and the quadrupolar nuclei [191]Ir (37.3% abundant, $I = 3/2$) and [193]Ir (62.7% abundant, $I = 3/2$). This effect will only be significant when the metal has isotopes which are abundant and have large quadrupole moments and/or small gyromagnetic ratios. As a result, this effect in transition metal carbonyl clusters has been predicted to be most prominent for Ir and less important for Co. However, for cobalt clusters the situation is further complicated by the occurrence of facile CO-exchange processes both in solution and the solid state. Nevertheless, it is important to note that the quadrupole coupling constant depends both on the nuclear quadrupole moment and the electric field gradient. Thus, there is a strong dependence on the symmetry of the metal sites which in turn influence the electric field gradients and, for metal sites with high symmetry, the electric field gradient should approach zero (in the case of cubic symmetry) resulting in little quadrupolar broadening.

The structure and dynamics of $[Co_4(CO)_{12}]$ have been contentious for some time partly because of the problems associated with quadrupolar interactions and their effect on NMR spectra and also because of the disorder found in the solid state by X-ray crystallography.[18] Nevertheless, ^{17}O NMR spectra clearly established the C_{3v} structure of $[Co_4(CO)_{12}]$ in solution[19] but interpretation of ^{13}C and [59]Co solution data proved less straightforward.[8] In solution, there are two [59]Co resonances due to the apical and basal cobalts but difficulties are experienced in obtaining the expected integration (1 : 3 respectively).[20] However, solid state [59]Co NMR measurements confirm that the low field resonance is due to Co_{apical} and is invariant with temperature whereas the Co_{basal} resonance at high field moves progressively to lower field with increasing temperature.[7,9]

^{13}C NMR measurements on $[Co_4(CO)_{12}]$ in solution show that the bridge/terminal COs undergo fast exchange[15,20–22] but ^{13}C MAS spectra reported for $[Co_4(CO)_{12}]$ are surprisingly different;[7,9,23–25] variable temperature measurements in the solid state are consistent with the occurrence of some movement but there have been different explanations as to whether the movement involves CO and/or Co movements about C_2 or C_3 axes. At $+75$ °C ^{13}C MAS NMR spectra still show the presence of the bridging CO resonance at δ 225 and it thus appears unlikely that there is exchange of bridge/terminal COs at this temperature.[9] The dynamics are better determined by [59]Co NMR and, above -23 °C, there is a rapid reorientation of the Co_4 tetrahedron from [59]Co T_1 measurements. Since the room temperature values of the nuclear quadrupole coupling constants (15 ± 3, 9 ± 2 MHz) and the asymmetry parameters (0.8, 0) for the apical and basal cobalts are different, this strongly supports a *reorientation* about *one* axis only, *viz.* the pseudo-C_3 axis which incorporates Co_{apical}. We envisage this motion (see Fig. 1) to involve a 120° or C_3 jump of the Co_4 tetrahedron within the carbonyl polyhedron about the pseudo C_3 axis and occurs with an activation energy of 40 ± 5 kJ mol^{-1}. The timescale of this motion can be estimated to be
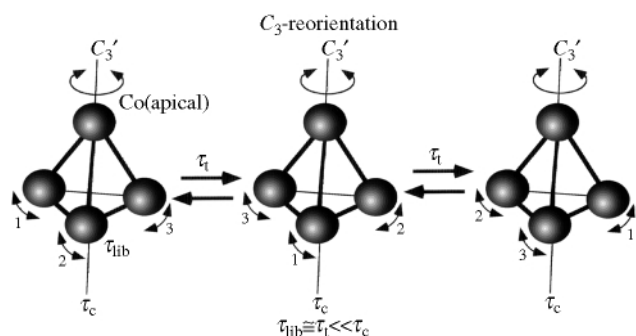

Fig. 1 Reorientation and libration of the Co_4 tetrahedron about the C_3 axis involving the apical Co in $[Co_4(CO)_{12}]$.

0.1–10 ms from the observed line broadening in the solid state ^{13}C MAS NMR spectrum.[7,9]

This motion is consistent with the ligand polyhedral model[26] and a recent structural redetermination of $[Co_4(CO)_{12}]$ at both 120 K and ambient temperature shows that at ambient temperature there are four disordered orientations of the Co_4 tetrahedron which are related by rotations about one of the fivefold axes of the ligand icosahedral polytope whereas at 120 K there are only two disordered orientations.[27] A facile interconversion between the major and minor orientations observed at 120 K allows a ready explanation of the observed ^{13}C and [59]Co solid state NMR results.[7,9]

3 Anionic clusters containing only carbonyls

Much shorter carbonyl T_1 values are found for anionic carbonyl clusters and ^{13}C cross polarisation (CP), magic angle spinning (MAS) NMR spectra with excellent signal-to-noise ratio can be obtained even at natural abundance levels of [13]CO if the cation is NMe_4^+.[28] This important result, which is a consequence of the combined effects of very rapid motion of the small spherical cation and the site symmetry of the anion, makes studies in this area much easier. Nevertheless, detailed interpretation of the ^{13}C CP/MAS spectrum still relies heavily upon prior knowledge of the crystal structure of the appropriate salt since, as noted above for neutral clusters, an isotropic ^{13}C chemical shift is usually observed for each crystallographically distinct CO site.

The isotropic ^{13}C chemical shift data observed for anionic carbonyl clusters in the solid state and in solution are shown in Table 2 and are entirely consistent with the structures determined by X-ray crystallography. The solid state NMR measurements on anionic clusters containing only carbonyls which have been reported so far show that there is no evidence for CO fluxionality in the solid state; nevertheless, it would be worthwhile investigating the ^{13}C CP/MAS NMR spectra of anionic carbonyl clusters which are known to be highly fluxional in solution. For example $[Rh_6(CO)_{15}]^{2-}$, which exhibits complete CO fluxionality over the Rh_6 octahedron at -70 °C,[13] and $[Rh_6C(CO)_{13}]^{2-}$;[31] in the latter case seven COs migrate around a Rh_4-square plane of the octahedron at -70 °C in solution and detailed X-ray measurements show that these same COs also exhibit extensive vibrational motion within the same Rh_4-square plane in the solid state.[32]

4 Carbonyl clusters containing hydride(s) and/or other ligands

The clusters containing only hydride(s) and CO, which have been examined by solid state NMR, are shown in Table 3 and include both neutral and anionic carbonyl clusters. The first four clusters in Table 3 have all been studied by neutron diffraction and shown to contain an interstitial hydride in an octahedral metal cavity. The values of $\delta(^1H)$ for the hydride resonance are similar in the solid state to those found in solution, with the exception of $[HCo_6(CO)_{15}]^-$ (see Table 3). In this case, the low field value in solution ($\delta +23$) supports Chini's original suggestion[36,50] that there is rapid hydride migration from inside to outside the cluster. This rearrangement in solution was originally proposed because the ^{1}H resonance of $[HCo_6(CO)_{15}]^-$ is only observed in protio-solvents, and at low temperature. It was assumed that at low temperature the rate of exchange from inside to outside the Co_6 octahedron is slow and the low field chemical shift is consistent with the presence of a H^+ which is associated with the COs (see Fig. 2). At higher temperatures in solution exchange results in loss of the proton signal.

Furthermore, the progressive shift of $\delta(^1H)$ from low to high field in the solid state correlates with an increasing displacement of the interstitial hydride from the centre of the

Table 2 Solution and solid state ^{13}CO chemical shifts for anionic carbonyl clusters containing ≥4 metal atoms

| Cluster | Site | Solid state NMR | | Expected relative intensities from X-ray data | | Solution NMR | |
		Ref.	$\delta(CO)^a$	Solid	Solution	$\delta(CO)^a$	Ref.
$[Ni_6(CO)_{12}]^{2-\,b}$	Terminal	28	200.6(6)	6	6	196.3(6)	29
	μ		239.0(6)	6	6	237.0(6)	
$[Ni_6(CO)_{12}]^{2-\,c}$	Terminal	28	200.0(2), 199.3(2), 198.5(2)	2:2:2	6		
	μ		239.5(2), 238.0(2), 235.4(2)	2:2:2	6		
$[Rh_6C(CO)_{15}]^{2-\,d}$	Terminal	9	197.7(6)	2:2:2	6	196.9(6)	30
	μ^e		242.7(1), 239.1(2)	1:2	3	235.4(3)	
	μ^f		231.4(2), 223.0(4)	2:2:2	6	224.0(6)	

^{a} Numbers in parentheses indicate relative intensities. ^{b} NMe_4^+ salt. ^{c} $N(PPh_3)_2^+$ salt. ^{d} NMe_3Bz^+ salt. ^{e} Inter-triangular. ^{f} Intra-triangular.

Table 3 Solid and solution ^1H NMR data on carbonyl clusters containing hydride(s) together with references to their neutron and X-ray diffraction structures

| Cluster | Ref. to diffraction data | | $\delta(^1H)^a$ | |
	Neutron	X-Ray	Solid	Solution
$[HRu_6(CO)_{18}]^-$	33		ca. 17 [34]	16.4 [33,35]
$[HCo_6(CO)_{15}]^-$	36		1 [34]	23.2 [b,36]
$[HNi_{12}(CO)_{21}]^{3-}$	37	37, 38	−26.8 [34]	−24.4 [37,39]
			−25.8 [38]	−24.2 [38]
$[H_2Ni_{12}(CO)_{21}]^{2-}$	37	37, 38	−19.9 [34]	−18.3 [37]
			−18.3(1), −19.3(1) [38]	
$[H_2Rh_{13}(CO)_{24}]^{3-}$	40	41	−26.0(1), −27.8(1) [34]	−27.0(1), −27.9(1) [c,42]
$[H_3Rh_{13}(CO)_{24}]^{2-}$		43	−28.1(1), −31.6(2) [34]	−28.2(1), −31.1(2) [d,42]
$[H_4Ru_4(CO)_{12}]$		44	ca. −18 [45,46]	−17.6 [47,48]
$[H_4Ru_4(CO)_{11}\{P(OMe)_3\}]$			ca. −18 [46]	−17.5(1), [e] −18.1(1) [47]
$[Ru_2Rh_2H_2(CO)_{12}]$		49	−19.5(1), [f] 21.6(1) [g,34]	−19.2(1), [f] −21.3(1) [g,h,49]

^{a} Figures in parentheses are relative intensities. ^{b} Below −50 °C in protio-solvents. ^{c} The resonances are not well resolved since the hydrides are still exchanging at −95 °C. ^{d} At −90 °C. ^{e} At −25 °C this resonance is a doublet due to $^2J(P–H) = 12.5$ Hz. ^{f} Due to RuHRh. ^{g} Due to RuHRu. ^{h} At −30 °C.
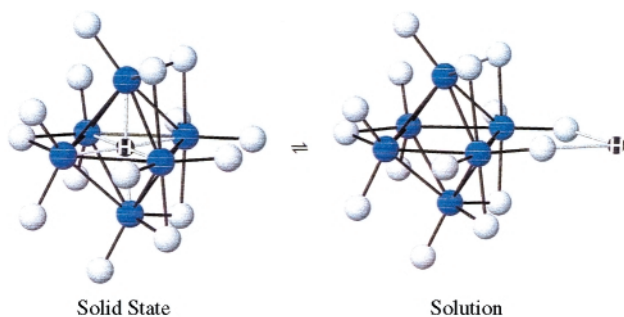
Fig. 2 Neutron diffraction (solid state) structure of $[HCo_6(CO)_{15}]^-$ and the hydride migration found in solution. The 2 terminal COs are almost parallel to each other on adjacent $Co(CO)_2$ groups; this results in a lengthening of the associated Co–Co edge in the solid state.

Table 4 Metal–hydrogen distances and solid-state chemical shifts of carbonyl clusters containing interstitial hydrides

Cluster	Average $d(M–H)^a$/pm	$\delta(^1H)$
$[HRu_6(CO)_{18}]^-$	203.7 (6)	+15.5
$[HCo_6(CO)_{15}]^-$	180.3 (4)	+1
	186.3 (2)	
$[H_2Ni_{12}(CO)_{21}]^{2-}$	184.5 (6)^b	−19.9
	200 (6)	
$[HNi_{12}(CO)_{21}]^{3-}$	172 (3)^b	−26.8
	222 (3)	

^{a} The values in parentheses indicate the number of M–H interactions. ^{b} These values are associated with the central Ni_3 triangle in the central Ni_6 layer.

octahedral metal cavity and a decrease in the symmetry of both the M_6 octahedron and of the carbonyl distribution around the metal cavity (see Table 4).[34,50] These results are also consistent with surface harmonic theory.[51]

The D resonance is extremely sensitive to site symmetry and, for $[DRu_6(CO)_{18}]^-$, a very sharp ($v_{1/2}$ 2 kHz) resonance is observed due to D being at the centre of a symmetrical octahedron.[34] Increasing displacement from the centre of the octahedron results in an increase of $v_{1/2}$ for the D resonance; for $[H_2Ni_{12}(CO)_{21}]^{2-}$, in which there is a large displacement of the H/D towards the central Ni_6 layer (see Table 4 and Fig. 3), no D resonance could be observed. It also appears from solid state NMR studies that there is little H/D movement within the Co_6 cavity. Thus, the neutron structure of $[HCo_6(CO)_{15}]^-$ shows that there are four short and two long Co–H distances, but over the temperature range (150 to 300 K) there is little change in $v_{1/2}$ of the D resonance.[34]

Owing to efficient cross polarisation transfer from the cation, recent work [38] on $[NMe_4]_2[H_2Ni_{12}(CO)_{21}]$ has allowed high quality ^1H and ^{13}C solid state spectra to be obtained. It is worthwhile noting that the hydride resonance could not be observed for $[H_2Ni_{12}(CO)_{21}]^{2-}$ when using the salts of $N(PPh_3)_2^+$ or NMe_3Bz^+ due to the overlapping cation resonances. Consistent with the crystal structure of $[NMe_4]_2[H_2Ni_{12}(CO)_{21}]$, which shows that four of the bridging COs on the inner layer (B_i) are displaced from the central Ni_6 plane and the two other B_i COs in the opposite direction (see Fig. 4), the solid state ^1H NMR of $[NMe_4]_2[H_2Ni_{12}(CO)_{21}]$ shows the presence of two high field resonances (see Table 3) due to the interstitial hydrides in the upper and lower octahedral cavities which have become inequivalent due to the displacements of the B_i COs from the central Ni_6 layer; this suggests that both the interstitial hydrides are on the plane of symmetry within the molecule otherwise a more complicated spectrum would have been observed. The ^1H
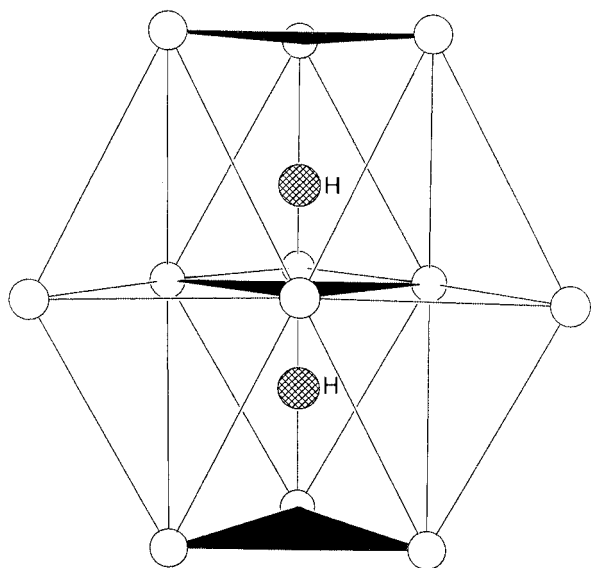
Fig. 3 Interstitial H-site occupancy in the Ni$_6$-octahedral cavity found by neutron diffraction for [H$_x$Ni$_{12}$(CO)$_{21}$]$^{(4-x)-}$ (x = 1 or 2).

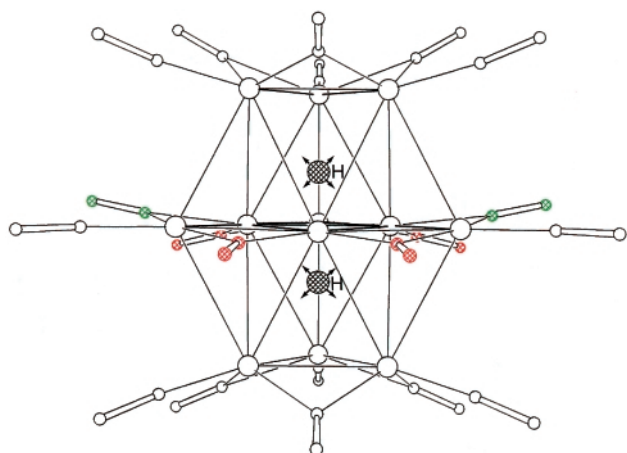**Fig. 4** Hydride oscillation about the plane of symmetry in [H$_2$Ni$_{12}$-(CO)$_{21}$]$^{2-}$.

NMR spectrum is unchanged over the temperature range 205 to 298 K but coalesces into a single resonance at 340 K. Since the ^{13}C NMR spectrum, which is entirely consistent with the solid state structure, and shows separate resonances for each of the symmetry related B$_i$ COs, remains unchanged over this temperature range, it would appear that the interstitial hydrides oscillate about the plane of symmetry (see Fig. 4) rather than an oscillation of the B$_i$ COs which would also produce equivalent hydrides. The mean value of the solid state values of δ(CO) compares favourably with those found in solution. For [HNi$_{12}$-(CO)$_{21}$]$^{3-}$ solution ^{13}C NMR measurements only showed the presence of one set of terminal and bridging outer layer resonances (T$_o$ and B$_o$ respectively) despite each of the outer layers being inequivalent because of the presence of only one interstitial hydride. As a result, it was difficult to be sure whether or not this arose because of accidental coincidence or because of hydride migration from the occupied to unoccupied interstitial site similar to the interstitial migration observed in solution for [H$_x$Rh$_{13}$(CO)$_{24}$]$^{(5-x)-}$ (x = 1–4)[42] and [HRh$_{14}$(CO)$_{25}$]$^{3-}$.[52] However, the solid state ^{1}H NMR spectrum of [HNi$_{12}$(CO)$_{21}$]$^{3-}$ is invariant with temperature (190 to 340 K) and suggests that there is little hydride movement in the solid state. The crystal structure of [NMe$_4$]$_3$[HNi$_{12}$(CO)$_{21}$] shows that the B$_i$ COs are again displaced from the central Ni$_6$ layer but the distortion is different to that found for the dihydride structure; one B$_i$ CO is significantly displaced towards the hydride, three are almost
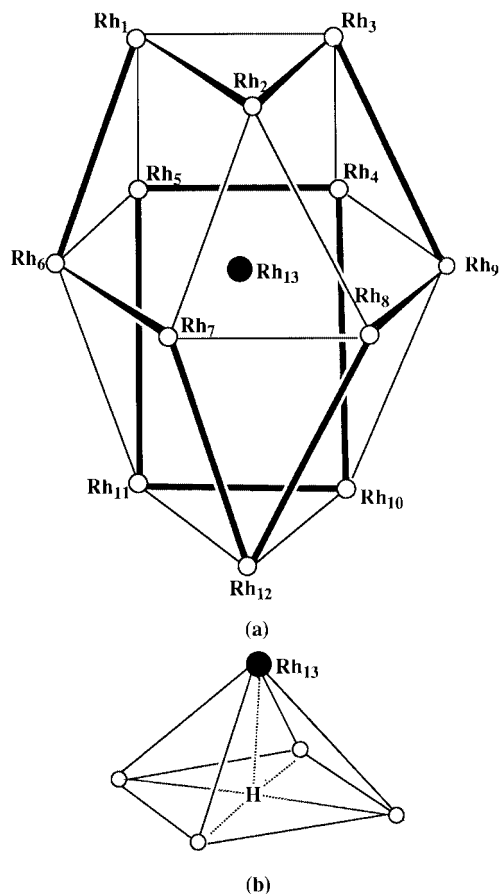

Fig. 5 (a) Schematic structure of [H$_x$Rh$_{13}$(CO)$_{24}$]$^{(5-x)-}$ (x = 1, 2 or 3). ● = Interstitial Rh, ○ = Rh(CO$_{term}$), ■ = μ-CO. In all cases, one H is associated with the Rh^{1}Rh^{3}Rh^{4}Rh^5 square face and, when x = 2, the other H is associated with the Rh^{8}Rh^{9}Rh^{10}Rh^{12} square face and, when x = 3, the additional H occupies the symmetry related Rh^{6}Rh^{7}Rh^{11}Rh^{12} square face. (b) Both Hs are *coplanar* with the outer Rh$_4$-square faces in the neutron diffraction structure of [H$_2$Rh$_{13}$(CO)$_{24}$]$^{3-}$.

coplanar with the central Ni$_6$ layer and the other two B$_i$ COs are in intermediate positions. Nevertheless, the solid state ^{13}C NMR is consistent with the solid state structure and, in this case, there is some broadening of the ^{13}C resonances due to the B$_i$ COs as a result of their oscillation about the central Ni$_6$ layer on increasing the temperature from 231 to 298 K.

The crystal structures of [H$_x$Rh$_{13}$(CO)$_{24}$]$^{(5-x)-}$ (x = 1–3)[41,43,53] are very similar; analysis of these structures suggested that hydride occupancy of square faces of the hexagonal close packed skeleton occurred and this was facilitated most easily in square faces which could more easily expand (*i.e.* contained the lowest number of μ-COs). Recently, neutron diffraction studies[40] on [H$_2$Rh$_{13}$(CO)$_{24}$]$^{3-}$ have confirmed this and show that both hydrides are coplanar with a Rh$_4$-square face (see Fig. 5). This H-site occupancy resembles the generally accepted location of H on a Rh(100) surface. Although the detailed geometry of H on a Rh(100) surface has not been experimentally established, hydride occupancy of such high co-ordination sites is the most energetically favourable[54] and there are some vibrational[55] and theoretical[56] studies to support this view.

In solution ^{1}H NMR studies showed that at room temperature there is facile (≤36.1 kJ mol^{-1}) H-migration *within* the Rh$_{13}$ skeleton for all the above clusters, together with exchange of 21 of the 24 COs around the outside of the cluster.[42] These motions have the effect of making all the outer triangular Rhs on the top and bottom layer equivalent and all those on the inner hexagonal layer equivalent. As a result the ^{1}H NMR spectra at room temperature of [H$_x$Rh$_{13}$(CO)$_{24}$]$^{(5-x)-}$ (x = 1–4) all consist of a well resolved doublet, due to coupling

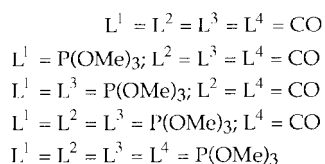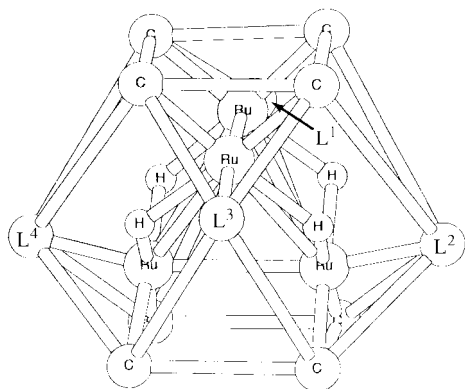$L^1 = L^2 = L^3 = L^4 = CO$

$L^1 = P(OMe)_3; L^2 = L^3 = L^4 = CO$

$L^1 = L^3 = P(OMe)_3; L^2 = L^4 = CO$

$L^1 = L^2 = L^3 = P(OMe)_3; L^4 = CO$

$L^1 = L^2 = L^3 = L^4 = P(OMe)_3$

Fig. 6 Schematic representation of the H_4Ru_4 group within the CO polyhedron of $[H_4Ru_4(CO)_{12-x}L_x]$ ($x = 0$–4; L = P(OMe)₃).

to the interstitial Rh, of septets of septets due to couplings to the hexagonal and outer triangular Rhs. Since the coupling of the interstitial Rh is of the order found for ^1J(Rh–H) (*ca.* 20 Hz), whereas the coupling to all the outer Rhs is much smaller, H-migration occurs *interstitially* giving a time-averaged, smaller, coupling to all the outer Rhs.[42] It was possible at low temperature to freeze both the H and CO motion for $[H_3Rh_{13}(CO)_{24}]^{2-}$ allowing detailed assignments to be made which supported the solid state diffraction measurements described above. For $[H_2Rh_{13}(CO)_{24}]^{3-}$ well resolved spectra due to the static structure could not be obtained at low temperature, suggesting a lower activation energy for H-migration.

In the solid state, however, the ^1H NMR spectra (≤ 340 K) of $[H_xRh_{13}(CO)_{24}]^{(5-x)-}$ ($x = 2$ or 3) are both consistent with the static structures. Thus, interstitial H-migration is much more difficult in the solid than in solution. In solution, H and CO migration appear to be concomitant and it is probable that interstitial H-migration is facilitated by the CO migration which induces slight deformations of the Rh_{13} skeleton; in the solid state, because of the much higher energies required to obtain a similar CO movement to that found in solution, neither CO nor H migration in $[H_xRh_{13}(CO)_{24}]^{(5-x)-}$ ($x = 2$ or 3) occurs.

The structures of $[H_4M_4(CO)_{12-x}L_x]$ (M = Ru or Os; $x = 0$–4; L = PR₃ or P(OR)₃) have been reviewed[57] and neutron diffraction data are only available on $[H_4Os_4(CO)_{11}\{P(OMe)_3\}]$[58] and $[H_4Ru_4(CO)_8\{P(OMe)_3\}_4]$.[59] In both cases the hydrides occupy the four long edges of the M_4 tetrahedron and HYDEX[60] has been used indirectly to locate the hydrides from X-ray diffraction studies of related clusters. In all cases there is a pseudo-D_{2d} H_4M_4 core and progressive CO substitution by other ligands occurs first on different metals *trans* to the non-H-bridged metal–metal vector and *transoid* to each other (see Fig. 6).

In solution there is rapid intramolecular H-exchange for $[H_4Ru_4(CO)_{11}\{P(OMe)_3\}]$ at room temperature since the ^1H resonance consists of a single resonance with a time-averaged coupling to ^{31}P; at 149 K there are two equally intense ^1H resonances ($\delta(^1H)$ −17.5 (s); −18.1 (d), ^2J(P–H) 12.5 Hz) consistent with the solution structure of $[H_4Ru_4(CO)_{11}\{P(OMe)_3\}]$ being the same as the solid state structure of $[Os_4H_4(CO)_{11}\{P(OMe)_3\}]$ which was determined by neutron diffraction.[57] The activation energy for H-movement from occupied to unoccupied edges over the Ru_4 tetrahedron in $[H_4Ru_4(CO)_{11}\{P(OMe)_3\}]$ in solution is 14.2 kJ mol⁻¹.[61]

Variable temperature, MAS and wide line solid state NMR

Table 5 Values of E_a for hydride migration in $[H_4Ru_4(CO)_{12-x}L_x]$ ($x = 0$ or 1; L = P(OMe)₃) and $[Ru_2Rh_2H_2(CO)_{12}]$ in the solid state, see text for explanation

| Cluster | E_a/kJ mol⁻¹ | | Ref. |
	$\Delta\nu_{1/2}$	T_1	
$[H_4Ru_4(CO)_{12}]$	75.1	59.2	45
		32 [a]	
	18.5 ± 2	16.1 ± 0.5	46
$[H_4Ru_4(CO)_{11}\{P(OMe)_3\}]$		15.8 ± 0.5	46
$[Ru_2Rh_2H_2(CO)_{12}]$		*ca.* 1	34

[a] Recalculation[46] using the T_1 data from ref. 45.

measurements have been carried out on $[H_4Ru_4(CO)_{12}]$ and $[H_4Ru_4(CO)_{11}\{P(OMe)_3\}]$.[46] The variations of spin–lattice relaxation time (T_1) and half linewidth of the hydride resonance with temperature for both samples are similar and suggest a common H-movement in the solid state with $E_a = 17 \pm 2$ kJ mol⁻¹. The similarity of these values from MAS and wide line measurements and the gross difference from earlier reported data[45] on $[H_4Ru_4(CO)_{12}]$ (see Table 5) deserves comment.

First, the sample of $[H_4Ru_4(CO)_{12}]$ used by Harding *et al.*[46] contained much less solvent of crystallisation than that used by Aime *et al.*,[45] allowing higher quality data to be obtained from wide line measurements. Secondly, the recalculation of E_a[46] using Aime's data from T_1 measurements[45] gives a much smaller value (see Table 5) and this is closer to that obtained by Harding *et al.*[46] for $[H_4Ru_4(CO)_{12-x}\{P(OMe)_3\}_x]$ ($E_a = 17 \pm 2$ kJ mol⁻¹ for $x = 0$ or 1). This implies that both the unsubstituted and mono-phosphite substituted clusters undergo a common H-movement, which is suggested to involve a correlated 2-site H-flip (see Fig. 7).[46] In the static structure it is probable that the edge-bridging hydrides in $[H_4Ru_4(CO)_{12-x}\{P(OMe)_3\}_x]$ ($x = 0$ or 1) are located as found by neutron diffraction for $[H_4Os_4(CO)_{11}\{P(OMe)_3\}]$. By analogy, the plane incorporating the *centre* of the Ru_4 tetrahedron and the 2 Rus on a long edge (H-bridged) is coplanar with the plane incorporating the same two Rus and the H (a in Fig. 7). As a result, the correlated motion involves a H-flip to enable the HRu_2 plane to become coplanar with adjacent Ru_3 faces (Fig. 7). This flip is also supported by the similarity of the calculated and experimentally observed values of T_{1min} in $[H_4Ru_4(CO)_{12}]$.

For the isoelectronic cluster $[Ru_2Rh_2H_2(CO)_{12}]$ multinuclear NMR measurements in solution have established the structure shown in Fig. 8.[49] At −30 °C the structure is static but with increasing temperature H(1) first oscillates between the Ru(1)–Rh(2) and Ru(1)–Rh(1) edges and then exchanges with H(2), resulting in broadening of the resonances associated with H(1) and H(2).[49]

In the solid state there are clearly two resonances due to H(1) and H(2) which have chemical shifts very similar to those observed at low temperature in solution. T_1 Measurements with MAS enabled the residual solvent in the crystal to be differentiated from the hydrides and variable temperature measurements showed that there is a weak temperature dependence of T_1 for the hydrides with E_a *ca.* 1 kJ mol⁻¹.[34] This could be due to one or both of the hydrides oscillating as shown in Fig. 7 or, since the M–H distances are significantly different (d(Ru1–H2) 1.452, d(Ru3–H2) 1.595, d(Ru1–H1) 1.664, d(Rh2–H1) 1.763 Å), an oscillation to equalise d(M–H) while remaining coplanar with the corresponding M_3 triangle, as found by X-ray analysis.[49,62]

5 Conclusion

In the absence of twinning and problems associated with disorder, solid state ^1H and ^{13}C NMR spectra of transition metal carbonyl clusters can usually be correlated exactly with the
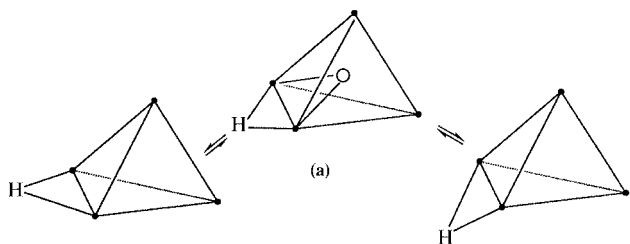
Fig. 7 2-Site H-flip about a Ru–Ru edge of the Ru$_4$ tetrahedron in [H$_4$Ru$_4$(CO)$_{12-x}$L$_x$] ($x = 0$ or 1; L = P(OMe)$_3$). The neutron diffraction structure of the analogous cluster [H$_4$Os$_4$(CO)$_{11}${P(OMe)$_3$}] shows that structure (a) is adopted in which the Ru$_2$H triangle is coplanar with the Ru$_2$O triangle where $\bigcirc$ = the centre of the Ru$_4$ tetrahedron.
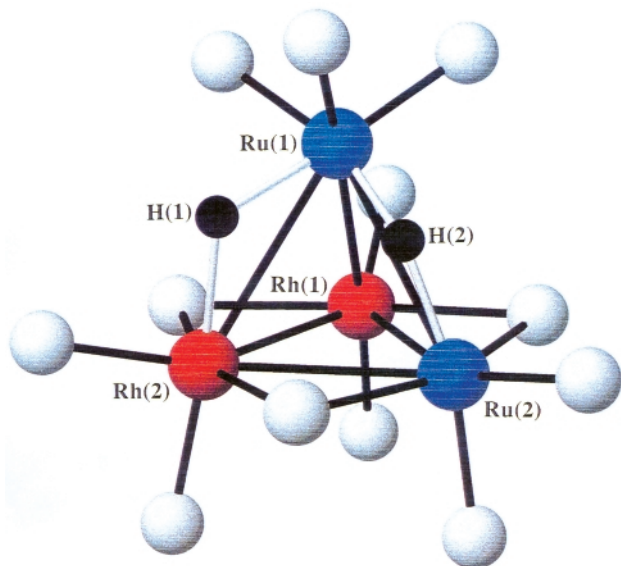

Fig. 8 Schematic structure of [Ru$_2$Rh$_2$H$_2$(CO)$_{12}$].

crystal structure since there is a resonance for each crystallographically distinct site. However, broader resonances are observed for metal clusters when the metal has isotopes which are abundant and have large quadrupole moments and/or small gyromagnetic ratios (*e.g.* ^{59}Co, ^{191}Ir, ^{193}Ir). The average isotropic chemical shift observed in the solid state for symmetry-related groups in the individual cluster is similar to that observed for the same group in solution.

^{13}C NMR spectra of anionic clusters can be obtained at natural ^{13}CO abundance using NMe$_4^+$ salts due to efficient cross-polarisation transfer. From ^{13}C NMR measurements in the solid state there is presently little evidence for any CO migration, except for [Co$_4$(CO)$_{12}$]. In this case the dynamics are better determined by ^{59}Co NMR measurements which show that there is a rapid *reorientation* of the Co$_4$ tetrahedron by 120° jumps about the pseudo-C_3 axis which incorporates Co$_{apical}$. This is the only case for which there is *direct evidence* for such a motion, although it has often been invoked to rationalise the dynamics observed for other clusters.

Many examples are now known for H-migration *over* the periphery of the metallic skeleton and *within* the metallic skeleton in solution. However, in the solid state, H-migration appears to be much more restricted, although H-oscillation from one plane to another about the same edge or through equalisation of d(M–H) for asymmetrically bridged hydrides has been observed.

The values of δ(H) for interstitial hydrides, which have been characterised by neutron diffraction, cover an enormous range (+15.5 to −26.8); the low field resonance results when H is at the centre of a regular metal octahedron and with increasing displacement of H from the centre of the octahedron and reduction in symmetry of the octahedron there is a progressive shift to high field.

7 References

1 K. Wade, *Adv. Inorg. Chem. Radiochem.*, 1976, **18**, 1.
2 D. M. P. Mingos and D. J. Wales, *Introduction to Cluster Chemistry*, Prentice Hall Int. Inc., Englewood Cliffs, NJ, 1990.
3 B. T. Heaton, J. A. Iggo, I. S. Podkorytov, D. J. Smawfield and S. P. Tunik, *Metal Clusters in Chemistry*, eds. P. Braunstein, L. Oro and P. Raithby, Wiley-VCH, accepted for publication.
4 B. E. Mann, *J. Chem. Soc.*, *Dalton Trans.*, 1997, 1457.
5 B. F. G. Johnson, *J. Chem. Soc.*, *Dalton Trans.*, 1997, 1473.
6 L. J. Farrugia, *J. Chem. Soc.*, *Dalton Trans.*, 1997, 1783.
7 T. Eguchi, H. Nakayama, H. Ohki, S. Takeda, N. Nakamura, S. Kernaghan and B. T. Heaton, *J. Organomet. Chem.*, 1992, **428**, 207.
8 S. Aime, R. Gobetto, D. Osella, L. Milone, G. E. Hawkes and E. W. Randall, *J. Magn. Reson.*, 1985, **65**, 308.
9 B. T. Heaton, J. Sabounchei, S. Kernaghan, H. Nakayama, T. Eguchi, S. Takeda, N. Nakamura and H. Chihara, *Bull. Chem. Soc. Jpn.*, 1990, **63**, 3019.
10 B. T. Heaton, L. Strona, R. Della Pergola, L. Garlaschelli, U. Sartorelli and I. H. Sadler, *J. Chem. Soc.*, *Dalton Trans.*, 1983, 173.
11 T. H. Walter, L. Reven and E. Oldfield, *J. Phys. Chem.*, 1989, **93**, 1320.
12 G. F. Stuntz, Ph.D. thesis, University of Illinois, 1974.
13 B. T. Heaton, A. D. C. Towl, P. Chini, A. Fumagalli, D. J. A. McCaffrey and S. Martinengo, *J. Chem. Soc.*, *Chem. Commun.*, 1975, 523.
14 F. A. Cotton, L. Kruczynski, B. L. Shapiro and L. F. Johnson, *J. Am. Chem. Soc.*, 1972, **94**, 6191.
15 J. Evans, B. F. G. Johnson, J. Lewis, T. W. Matheson and J. R. Norton, *J. Chem. Soc.*, *Dalton Trans.*, 1978, 626.
16 D. Braga, *Chem. Rev.*, 1992, **92**, 633.
17 M. R. Churchill and J. P. Hutchinson, *Inorg. Chem.*, 1978, **17**, 3528.
18 C. H. Wei, *Inorg. Chem.*, 1969, **8**, 2384; F. H. Carré, F. A. Cotton and B. A. Frenz, *Inorg. Chem.*, 1976, **15**, 380.
19 S. Aime, D. Osella, L. Milone, G. E. Hawkes and E. W. Randall, *J. Am. Chem. Soc.*, 1981, **103**, 5920.
20 M. A. Cohen, D. R. Kidd and T. L. Brown, *J. Am. Chem. Soc.*, 1975, **97**, 4408 and refs. therein.
21 J. Evans, B. F. G. Johnson, J. Lewis and T. W. Matheson, *J. Am. Chem. Soc.*, 1975, **97**, 1245.
22 S. Aime and L. Milone, *Prog. NMR Spectrosc.*, 1977, **11** 183.
23 B. E. Hanson and E. C. Lisic, *Inorg. Chem.*, 1986, **25**, 716.
24 S. Aime, M. Botta, R. Gobetto and B. E. Hanson, *Inorg. Chem.*, 1989, **28**, 1196.
25 C. E. Anson, R. E. Benfield, A. W. Bott, B. F. G. Johnson, D. Braga and E. A. Marseglis, *J. Chem. Soc.*, *Chem. Commun.*, 1988, 889.
26 R. E. Benfield and B. F. G. Johnson, *J. Chem. Soc.*, *Dalton Trans.*, 1978, 1554; B. F. G. Johnson and Y. V. Roberts, *Polyhedron*, 1993, **12**, 977.
27 L. J. Farrugia, D. Braga and F. Grepioni, *J. Organomet. Chem.*, 1999, **573**, 60.
28 T. Eguchi, R. A. Harding, B. T. Heaton, G. Longoni, K. Miyagi, J. Nähring, N. Nakamura, H. Nakayama and A. K. Smith, *J. Chem. Soc.*, *Dalton Trans.*, 1997, 479.
29 G. Longoni, B. T. Heaton and P. Chini, *J. Chem. Soc.*, *Dalton Trans.*, 1980, 1537.
30 V. G. Albano, P. Chini, S. Martinengo, D. J. A. McCaffrey, D. Strumolo and B. T. Heaton, *J. Am. Chem. Soc.*, 1974, **96**, 8106.
31 B. T. Heaton, L. Strona and S. Martinengo, *J. Organomet. Chem.*, 1981, **215**, 415.
32 D. Braga and B. T. Heaton, *J. Chem. Soc.*, *Chem. Commun.*, 1987, 608.
33 P. F. Jackson, B. F. G. Johnson, J. Lewis, P. R. Raithby, M. McPartlin, W. J. H. Nelson, K. D. Rouse, J. Allibon and S. A. Mason, *J. Chem. Soc.*, *Chem. Commun.*, 1980, 295.
34 T. Eguchi, R. A. Harding, B. T. Heaton, G. Longoni, K. Myagi, J. Nähring, N. Nakamura, H. Nakayama, J. Pakkanen, J. Pursiainen and A. K. Smith, *J. Chem. Soc.*, *Dalton Trans.*, 1996, 625.

35 C. R. Eady, P. F. Jackson, B. F. G. Johnson, J. Lewis, M. Malatesta, M. McPartlin and W. J. H. Nelson, *J. Chem. Soc.*, *Dalton Trans.*, 1980, 383.

36 D. W. Hart, R. G. Teller, C.-Y. Wei, R. Bau, G. Longoni, S. Campanella, P. Chini and T. F. Koetzle, *J. Am. Chem. Soc.*, 1981, **103**, 1458.

37 R. W. Broach, L. F. Dahl, G. Longoni, P. Chini, A. J. Schulz and J. M. Williams, *Adv. Chem. Ser.*, 1978, **167**, 93.

38 J. V. Barkley, B. T. Heaton, L. Manzi, A. K. Smith, A. Steiner, H. Nakayama, K. Miyagi, R. Harding and T. Eguchi, *J. Organomet. Chem.*, 1999, **573**, 254.

39 A. Cerrioti, P. Chini, R. Della Pergola and G. Longoni, *Inorg. Chem.*, 1983, **221**, 1595.

40 R. Bau, M. H. Drabnis, L. Garlaschelli, W. T. Klooster, Z. Xie, T. F. Koetzle and S. Martinengo, *Science*, 1997, **275**, 1099.

41 V. G. Albano, G. Ciani, S. Martinengo and A. Sironi, *J. Chem. Soc.*, *Dalton Trans.*, 1979, 978.

42 C. Allevi, B. T. Heaton, C. Seregni, L. Strona, R. J. Goodfellow, P. Chini and S. Martinengo, *J. Chem. Soc.*, *Dalton Trans.*, 1986, 1375.

43 V. G. Albano, A. Ceriotti, P. Chini, G. Ciani, S. Martinengo and W. M. Anker, *J. Chem. Soc.*, *Chem. Commun.*, 1975, 859.

44 R. D. Wilson, S. M. Wu, R. A. Love and R. Bau, *Inorg. Chem.*, 1978, **19**, 271.

45 S. Aime, R. Gobetto, A. Orlandi, C. J. Groombridge, G. E. Hawkes, M. D. Mantle and K. D. Sales, *Organometallics*, 1994, **13**, 2375.

46 R. A. Harding, H. Nakayama, T. Eguchi, B. T. Heaton, N. Nakamura and A. K. Smith, *Polyhedron*, 1998, **17**, 2857.

47 S. A. R. Knox and H. D. Kaesz, *J. Am. Chem. Soc.*, 1971, **93**, 4594.

48 S. Aime and R. Gobetto, unpublished work cited in ref. 45.

49 J. Pursianen, T. A. Pakkanen, B. T. Heaton, C. Seregni and R. J. Goodfellow, *J. Chem. Soc.*, *Dalton Trans.*, 1986, 681.

50 P. Chini, G. Longoni, S. Martinengo and A. Ceriotti, *Adv. Chem. Ser.*, 1978, **167**, 1.

51 M. J. Duer and D. J. Wales, *Polyhedron*, 1991, **10**, 1749.

52 B. T. Heaton, C. Brown, D. O. Smith, L. Strona, R. J. Goodfellow, P. Chini and S. Martinengo, *J. Am. Chem. Soc.*, 1980, **102**, 6175.

53 G. Ciani, A. Sironi and S. Martinengo, *J. Chem. Soc.*, *Dalton Trans.*, 1981, 519.

54 K. Christmann, *Prog. Surf. Sci.*, 1995, **48**, 15; *Mol. Phys.*, 1989, **66**, 1.

55 L. J. Richter and W. Ho, *J. Vac. Sci. Technol. A*, 1987, **5**, 453.

56 D. R. Hamann and P. J. Feibelman, *Phys. Rev. B*, 1987, **37**, 3847; P. J. Feibelman and D. R. Hamann, *Surf. Sci.*, 1990, **234**, 377; P. J. Feibelman, *Phys. Rev. B*, 1991, **43**, 9452; D. Henning, S. Wilke, R. Löber and M. Methfessel, *Surf. Sci.*, 1993, **89**, 287.

57 R. Bau and R. G. Teller, *Struct. Bonding* (*Berlin*), 1981, **44**, 1.

58 C. Y. Wei, L. Garlaschelli, R. Bau and T. F. Koetzle, *J. Organomet. Chem.*, 1981, **213**, 63.

59 A. G. Orpen and R. K. McMullan, *J. Chem. Soc.*, *Dalton Trans.*, 1983, 463.

60 A. G. Orpen, *J. Chem. Soc.*, *Dalton Trans.*, 1980, 2509.

61 H. D. Kaesz, *Chem. Br.*, 1973, **9**, 344.

62 J. Pursianen and T. A. Pakkanen, *J. Chem. Soc.*, *Chem. Commun.*, 1984, 252.